Published online December 15, 2004

Nucleic Acids Research, 2004, Vol. 32, No. 22 ***e178***
doi:10.1093/nar/gnh177

Sigmoidal curve-fitting redefines quantitative real-time PCR with the prospective of developing automated high-throughput applications

R. G. Rutledge*

Natural Resources Canada, 1055 du P.E.P.S, Sainte-Foy, Quebec, Canada G1V 4C7

Received May 25, 2004; Revised October 15, 2004; Accepted November 24, 2004

ABSTRACT

Quantitative real-time PCR has revolutionized many aspects of genetic research, biomedical diagnostics and pathogen detection. Nevertheless, the full potential of this technology has yet to be realized, primarily due to the limitations of the threshold-based methodologies that are currently used for quantitative analysis. Prone to errors caused by variations in reaction preparation and amplification conditions, these approaches necessitate construction of standard curves for each target sequence, significantly limiting the development of high-throughput applications that demand substantive levels of reliability and automation. In this study, an alternative approach based upon fitting of fluorescence data to a four-parametric sigmoid function is shown to dramatically increase both the utility and reliability of quantitative real-time PCR. By mathematically modeling individual amplification reactions, quantification can be achieved without the use of standard curves and without prior knowledge of amplification efficiency. Combined with provision of quantitative scale via optical calibration, sigmoidal curve-fitting could confer the capability for fully automated quantification of nucleic acids with unparalleled accuracy and reliability.

INTRODUCTION

First introduced commercially in 1996, fluorescence-based detection of amplicon DNA allowed the kinetics of PCR amplification to be monitored in real time, providing the ability to quantify nucleic acids with extraordinary ease and accuracy (1–3). With a large dynamic range (7–8 magnitudes) and a high degree of sensitivity (1–5 molecules), quantitative real-time PCR has greatly impacted many aspects of genetic research, in addition to facilitating the development of new applications in biomedical diagnostics for pathogen detection, viral load, and minimal residual disease, and for gene expression analysis in relation to disease, pathogenesis and oncogenesis (4–9).

Despite the significance of this technology, its full potential has yet to be realized, primarily due to limitations associated with the threshold-based methodologies that currently predominate. Developed upon comparing amplification reactions at a point in which they have identical amounts of amplicon DNA, a theoretical 'threshold' cycle (C_t) is the primary quantitative output (10–12). Much of the technical limitation of the threshold approach is associated with conversion of C_t values into the number of target molecules that requires construction of a standard curve for each target sequence (12–14). Although standard curves can be effective, their construction requires extensive effort and is prone to errors in DNA standard preparation, which is further exacerbated by the difficulties of assessing accuracy-of-scale (5,15,16).

An alternative approach was recently proposed by Liu and Saint (17), in which a sigmoid function was shown to model PCR amplification more effectively than the exponential model upon which the threshold method is based. In the study presented here, the remarkable implications and quantitative effectiveness of sigmoidal modeling were examined in detail, which demonstrates that many of the limitations of the threshold method can be circumvented, including abrogating the need for standard curves. Most significant, however, is the potential to develop automated high-throughput applications for quantitative real-time PCR, with unprecedented capabilities for quality control over both PCR amplification and establishment of quantitative scale.

MATERIALS AND METHODS

Fluorescence datasets

All the fluorescence readings used in this study were obtained from a previous study, in which five replicate standard curves were constructed for each of two amplicons (K3/K2, 218 bp and K1/K2, 102 bp), with the smaller amplicon nested within the larger (18). In brief, PCR amplifications were conducted using QuantiTect™ SYBR® Green PCR Kit (Qiagen Inc.) according to the manufacturer's instructions, and an Opticon2 DNA Engine (MJ Research Inc.) with thermocycling initiated by a 15 min incubation at 94°C, followed by 45 cycles (90°C for 1 s; 62°C for 120 s) with a single fluorescent reading taken at the end of each cycle.

Specificity of amplification and absence of primer dimers was confirmed by melting curve analysis at the end of each run. To maintain consistency with the previously generated C_t data, fluorescence readings were exported after

*Tel: +1 418 648 2582; Fax: +1 418 648 5849; Email: Bob.Rutledge@NRCan.gc.ca

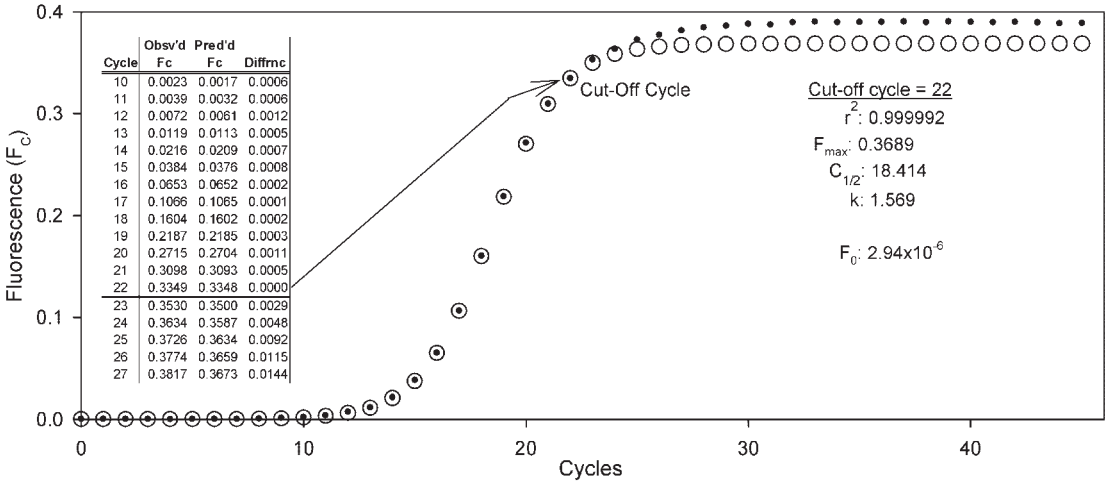

Figure 1. An example of modeling PCR amplification with a four-parametric sigmoid function (Equation 1). Curve-fitting of experimentally derived fluorescence dataset (Obsv'd F_C; dots) to Equation 1 generates values for three parameters (F_{max}, $C_{1/2}$ and k), from which the target quantity (F_0) can be calculated using Equation 2. Effectiveness of this sigmoidal model is illustrated by the F_C values generated by Equation 1 (Pred'd F_C; open circles) that agree within ±0.2% with the observed F_C, if cycles beyond the cut-off are excluded from the curve-fitting process (see Materials and Methods, and Supplementary Datasets 1 and 2 for additional details).

background subtraction via baseline averaging of the 5 cycles immediately preceding the cycles in which fluorescence was first detected, and data for each amplicon were exported to an Excel workbook for analysis (provided as Supplementary Datasets 1 and 2).

Curve-fitting

The nonlinear regression function of SigmaPlot (Version 8) was used to fit fluorescence readings to Equation 1. Following extensive analyses, it became evident that cycles within the plateau phase diverged significantly from that of predicted by sigmoidal modeling, an anomaly that impacted the effectiveness of the curve-fitting process. It was thus necessary to exclude plateau cycles, a process that was based upon selection of a cut-off cycle, beyond which cycles were excluded from the regression analysis (Figure 1; Supplementary Datasets 1 and 2). The criterion used for the selection of the cut-off cycle was developed upon subjecting each amplification curve to repetitive regression analyses, in which the last cycle was excluded and the regression analysis repeated. As best illustrated in the Excel workbooks provided as Supplementary Datasets 1 and 2, this generated a series of r^2, F_{max}, $C_{1/2}$ and k values, from which a F_0 value was calculated for each sequential data-subset using Equation 2. The impact of this sequential exclusion of cycles was then evaluated, which revealed a highly regular trend in which the calculated F_0 value reached a minimum, followed by a small but progressive increase (Figure 2). Selection of the cut-off cycle for all amplification curves was based upon the subset that produced the minimum-calculated F_0 value (for additional details see Supplementary Datasets 1 and 2).

RESULTS

Sigmoidal curve-fitting (SCF)

As previously described by Liu and Saint (17), real-time PCR can be effectively modeled using the four-parametric sigmoid function:

$$F_C = \frac{F_{max}}{1 + e^{-(C - C_{1/2}/k)}} + F_b, \quad \mathbf{1}$$

where C is cycle number, F_C is reaction fluorescence at cycle C, F_{max} is the maximal reaction fluorescence that defines the cessation of amplification, $C_{1/2}$ is the fractional cycle at which reaction fluorescence reaches half of F_{max}, k is the slope of the curve and F_b is the background reaction fluorescence. The central principle of the SCF method is the ability to describe individual PCR amplifications solely in terms of these four parameters, the values of which can be determined by fitting experimentally derived fluorescence readings to Equation 1 (17,19,20). Curve-fitting algorithms use a reiterative process that systematically changes the value of each variable such that correlation with the experimental data is maximized, a process that is repeated until a specified tolerance is satisfied.

The general efficacy of SCF for modeling of real-time PCR amplification can be demonstrated by the correlation of experimentally derived F_C datasets to that predicted by Equation 1. Indeed, extensive analyses confirmed that SCF is effective, producing correlation coefficients (r^2) that reach averages of about 0.99998 for highly replicated amplifications (n = 20), down to an average of about 0.99992 for individual amplification reactions (Supplementary Datasets 1 and 2; see below). An important exception, however, is evident in Figure 1, in that the reaction fluorescence produced within the plateau phase was found to diverge from that predicted by Equation 1. Although this anomaly is much less prevalent under high amplification efficiencies (data not shown), it was found necessary to exclude plateau cycles from the curve-fitting process through the selection of a cut-off cycle (Figure 1). Nonetheless, extensive application of SCF demonstrated a capacity to model real-time PCR with a truly remarkable degree of precision.

Of all the challenges encountered during development of the SCF method, developing a criterion for the selection of the cut-off cycle was the most difficult. An effective solution was

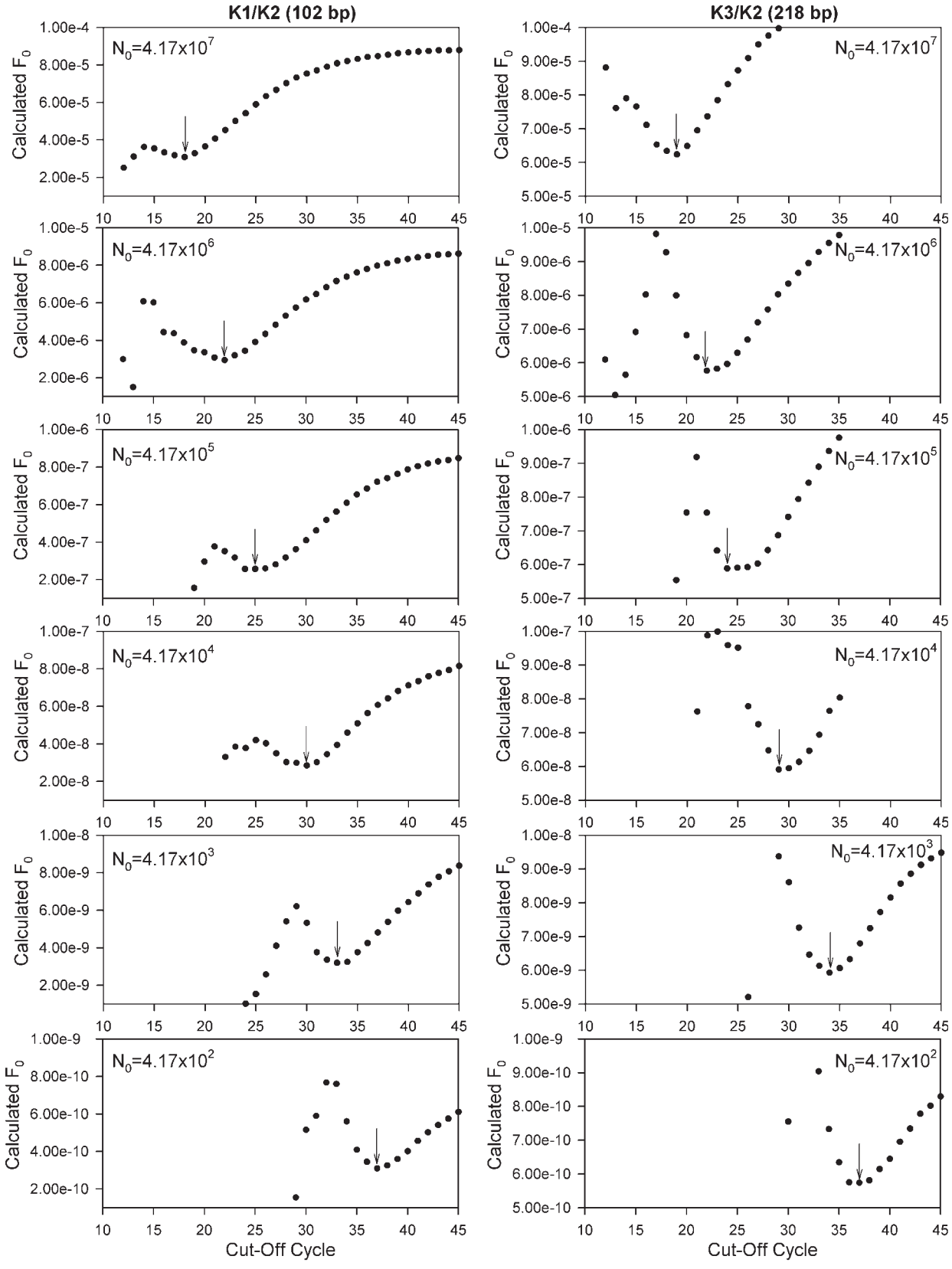

Figure 2. Selection of the cut-off cycle used for SCF quantification, based upon the minimum-calculated F_0. As described in Materials and Methods (with further details provided in Supplementary Datasets 1 and 2), each fluorescence dataset was subjected to repetitive curve-fitting during which the last cycle was sequentially removed. Plotting the resulting calculated F_0 values against cut-off cycle revealed a highly regular pattern, allowing SCF quantification to be based upon the cut-off cycle that produced the minimum F_0 value (arrow). The observed drift in calculated F_0 was related to a persistent increase in reaction fluorescence during the plateau phase of the amplification curve (see Figure 1 and text for additional details).

based upon the empirical observation that as cycles from the plateau were sequentially removed from the curve-fitting process, the resulting changes in F_0 value were found to be highly reproducible (Figure 2). Selection of the cut-off cycle for each target concentration was subsequently based upon that which produced a minimum F_0 value, as illustrated in Figure 2 (see Materials and Methods, and Supplementary Datasets 1 and 2 for additional details).

Quantitative precision of SCF

Previous quantitative methods have been based upon the direct relationship between the target quantity and the number of cycles needed to produce quantifiable amounts of amplicon DNA. An alternative approach is provided by a simple derivative of Equation 1, when $C = 0$:

$$F_0 = \frac{F_{\max}}{1 + e^{(C_{1/2}/k)}}, \quad \mathbf{2}$$

where F_0 is the target quantity expressed in fluorescence units (FU). It is important to note that F_0 is a bona fide quantitative entity, although expressed in arbitrary units that are unique to the instrumentation and the fluorescence chemistry employed for amplicon detection (SYBR® Green I in this study).

The SCF method presents two aspects of practical importance. First is the potential to conduct quantification without the knowledge of amplification efficiency, and second, that quantification and establishment of quantitative scale are separable processes. Thus, if sufficient levels of quantitative precision can be demonstrated, and if establishment of quantitative scale (i.e. fluorescence calibration) can be effectively achieved, SCF could provide capabilities either difficult to achieve or unattainable using a threshold approach.

A previous study in which the quantitative accuracy of the C_t method was examined provided an ideal dataset for evaluating the SCF method (18). Encompassing 10 standard curves constructed from replicate amplifications ($n = 4$) of six target concentrations, this earlier study generated a total of 120 amplification reactions for each of the two amplicons (K1/K2 = 102 bp and K3/K2 = 218 bp). In addition to providing a large number of amplification reactions from which fluorescence datasets could be obtained, this provided the ability to directly compare quantitative determinations generated by SCF and C_t methodologies. Owing to the large size of the datasets and extensive scope of the work, it is only possible to present summaries of the analyses. The reader is, however, referred to the Excel workbooks provided as supplementary data online (Supplementary Datasets 1 and 2), which contain the fluorescence readings along with the calculations and data compilations used to prepare the summaries presented in this report.

As a starting point for assessing quantitative precision, the relative differences in F_0 values derived from each of the six target quantities were examined for each of the two amplicons (Table 1). This indicated that a high level of precision can be achieved with SCF quantification, as reflected by the low variance from that of predicted (Table 1, ±3.0% and ±7.7% for K3/K2 and K1/K2, respectively), and that these are very similar to the variances produced by C_t-based quantification (±4.8% and ±10.0%, respectively, Supplementary Datasets 1 and 2).

The quantitative precision of SCF was further assessed by examining the relationship of F_0 to amplicon size, as based on the linear relationship between SYBR® Green I fluorescence and DNA mass; i.e. for an identical target quantity, the respective F_0 values for each amplicon should differ in direct relation to their size (218 bp versus 102 bp; ratio = 2.14). Indeed, the average F_0 values adjusted to the highest target quantity differ from theoretical value by only 6.8% (5.91×10^{-5} versus 2.95×10^{-5}, Table 1; ratio = 2.00). In addition to supporting the precision of SCF quantification, this further confirms that the fluorescence characteristics of these two amplicons are similar, as was previously concluded based upon their respective DNA mass at threshold (M_t, see below) that differ by 7.3% (18).

Establishment of quantitative scale via optical calibration

Conversion of F_0 to the number of target molecules would appear to be straightforward, accomplished by first correlating fluorescence to DNA mass such that:

$$M_0 = \mathrm{CF} \times F_0, \quad \mathbf{3}$$

where CF is a calibration factor, expressed in this study as the number of nanograms of double-stranded DNA per SYBR® Green I fluorescence unit (ng/FU), such that M_0 is the mass of the target quantity in nanograms of the double-stranded DNA. The M_0 of the target quantity can in turn be related to the number of target molecules, such that:

$$N_0 = \left(M_0 \times 9.1 \times 10^{11}\right)/\mathrm{A}_S, \quad \mathbf{4}$$

Table 1. Quantitative precision of SCF for two amplicons covering six magnitudes of target quantity

Predicted N_0[a]	K3/K2 (218 bp) F_0[b]	Percentage of predicted[c]	K1/K2 (102 bp) F_0[b]	Percentage of predicted[c]
4.17×10^7	6.24×10^{-5}	105.6	3.09×10^{-5}	104.6
4.17×10^6	5.76×10^{-6}	97.5	2.94×10^{-6}	99.7
4.17×10^5	5.88×10^{-7}	99.6	2.56×10^{-7}	86.8
4.17×10^4	5.90×10^{-8}	99.9	2.84×10^{-8}	96.2
4.17×10^3	5.93×10^{-9}	100.3	3.19×10^{-9}	108.0
4.17×10^2	5.74×10^{-10}	97.1	3.09×10^{-10}	104.7
Average[d]/±SD	5.91×10^{-5}	±3.0	2.95×10^{-5}	±7.7

[a]Predicted number of target molecules based upon dilution of a DNA standard quantified via A_{260}.
[b]Target quantity expressed in fluorescence units (Equation 2), derived from SCF of fluorescence readings averaged from replicate amplifications ($n = 20$).
[c]Relative to the average F_0 adjusted for dilution.
[d]Average F_0 adjusted for dilution relative to $N_0 = 4.17 \times 10^7$.

where N_0 is the initial number of target molecules, A_S is the amplicon size in base pairs and 9.1×10^{11} is the number of single base pair molecules per nanogram. Note that CF is the sole determinant of error in quantitative scale, and that it encompasses the optical characteristics of both the reaction mixture and instrumentation, providing what could be termed as 'optical calibration'.

Amplification of a quantified DNA standard provides a straightforward method for CF determination, based upon rearrangement of Equation 3:

$$CF_{SCF} = \frac{M_P}{F_0}, \quad \mathbf{5}$$

where CF_{SCF} is the SCF-based calibration factor, in which F_0 is target quantity in FU (Table 1) and M_P is the predicted mass of the target in nanograms derived from the predicted number of target molecules in the standard (Equation 4). Similarly, this approach can be extended to C_t-based quantification:

$$CF_{C_t} = \frac{M_t}{F_t}, \quad \mathbf{6}$$

where CF_{C_t} is the C_t-based calibration factor, M_t is amplicon DNA mass at threshold and F_t is the fluorescence threshold, in which M_t is derived from the number of amplicon molecules at threshold (N_t), which in turn is derived from the intercept of a C_t-based standard curve (18).

Table 2. Correlation of reaction fluorescence to target DNA mass

Predicted N_0[a]	K3/K2 CF_{SCF}[b] (ng/FU)	K1/K2 CF_{SCF}[b] (ng/FU)
4.17×10^7	160	151
4.17×10^6	173	159
4.17×10^5	170	182
4.17×10^4	169	165
4.17×10^3	169	147
4.17×10^2	174	151
Average ± CV[c]	169 ± 3.0%	159 ± 8.2%
CF_{Ct}[d]	164 ± 14.7%	177 ± 19.0%
Overall average ± CV	167 ± 4.6%	

[a]Predicted number of target molecules based upon dilution of DNA standard quantified via A_{260}.
[b]SCF-based calibration factor (M_P/F_0).
[c]Average ± coefficient of variation.
[d]Threshold-based calibration factor (M_t/F_t). See text for additional details.

The relative accuracies of SCF- and C_t-based quantification were assessed by comparing CF_{SCF} and CF_{C_t} generated for each of the two amplicons (Table 2). This revealed that each of the four quantitative scales agree within ±5%, supporting the effectiveness of these two diverse quantitative methods in relation to a shared DNA standard. The effectiveness of a common quantitative scale was further examined by converting F_0 and C_t values into the number of target molecules using the average CF derived in Table 2. This demonstrated that the combined variance in N_0 determination for both amplicons averaged ±6.4% from that of predicted over the six magnitudes of target quantity examined (Table 3).

Dynamics of amplification efficiency

A fundamental difference between exponential and sigmoidal models relates to the amplification efficiency, such that for threshold-based quantification, amplification efficiency is presumed to be constant (14,18), whereas under SCF quantification, amplification efficiency is dynamic. This can be illustrated with an equation described by Liu and Saint (17):

$$E_C = \frac{1 + e^{-(C-1-C_{1/2}/k)}}{1 + e^{-(C-C_{1/2}/k)}} - 1, \quad \mathbf{7}$$

where E_C is the amplification efficiency at cycle C. Under this definition, amplification efficiency decreases continuously throughout the amplification process, such that each cycle has a unique amplification efficiency (cycle efficiency or E_C). Furthermore, amplification efficiency can be traced back to the initiation of thermocycling, when $C = 0$:

$$E_0 = \frac{1 + e^{(1+C_{1/2}/k)}}{1 + e^{(C_{1/2}/k)}} - 1, \quad \mathbf{8}$$

where E_0 is defined in this study as the 'initial' amplification efficiency. Under this model, E_C is equal to E_0 at the initiation of thermocycling but progressively decreases during thermocycling which eventually leads to cessation of amplification as E_C approaches zero, marking entry into the plateau phase. Of practical significance, determination of E_0 allows monitoring of amplification efficacy within individual reactions, from which aberrant amplification reactions can be identified that would otherwise remain undetected using a threshold approach.

Table 3. Effectiveness of a common quantitative scale for SCF and C_t determinations

Predicted N_0[a]	K3/K2 C_t[b] (% of predicted)	SCF[c] (% of predicted)	K1/K2 C_t[b] (% of predicted)	SCF[c] (% of predicted)
4.17×10^7	106.4	104.4	101.2	110.3
4.17×10^6	101.5	96.4	96.7	105.4
4.17×10^5	98.3	98.4	90.9	91.7
4.17×10^4	94.0	98.8	78.2	101.6
4.17×10^3	105.1	99.1	105.1	114.1
4.17×10^2	105.4	96.0	99.1	110.6
Average ± SD[d]	101.8% ± 4.8	98.9% ± 3.0	95.0% ±9.5	105.6% ±8.1

[a]Predicted number of target molecules based upon dilution of DNA standard quantified via A_{260}.
[b]Average C_t ($n = 20$) converted to the number of target molecules (N_0) using the average CF from Table 2 (Supplementary Datasets 1 and 2).
[c]F_0 values from Table 1 converted into the number of target molecules (N_0) using the average CF from Table 2 (Equations 3 and 4).
[d]Standard deviation (average = 6.4%).

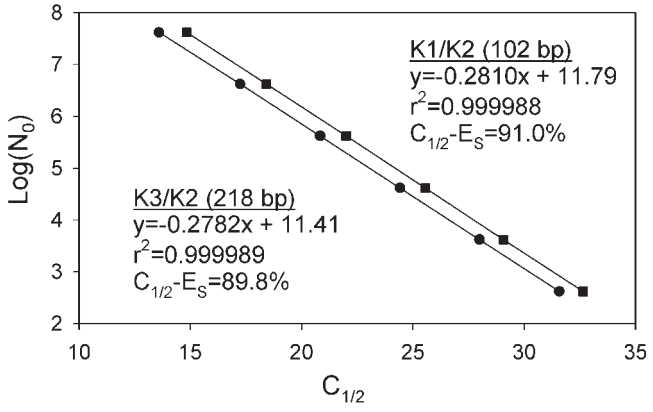

Figure 3. Linear relationship between Log(N_0) and $C_{1/2}$. Analogous to C_t-based standard curves used for absolute quantification under the threshold method, plotting $C_{1/2}$ against the log of target quantity produces a line, whose slope is related to the initial amplification efficiency and the intercept related to the quantity of amplicon at F_{max}.

Relating exponential and sigmoidal models

Quantification under the threshold method is based upon the exponential equation:

$$N_0 = \frac{N_t}{(E+1)^{C_t}}, \quad \textbf{9}$$

where N_t is the number of amplicon molecules at threshold and N_0 is the target quantity in molecules. A derivative of this equation describes the linear relationship between the log of target quantity and C_t which is the basis for standard curve construction (18):

$$\mathrm{Log}(N_0) = -\mathrm{Log}(E+1)C_t + \mathrm{Log}(N_t). \quad \textbf{10}$$

Analogy of C_t with $C_{1/2}$, can be demonstrated by plotting Log(N_0) against $C_{1/2}$, which also produces a line (Figure 3) such that:

$$\mathrm{Log}(N_0) = -\mathrm{Log}(E_0+1)C_{1/2} + \mathrm{Log}(N_{max}), \quad \textbf{11}$$

in which:

$$E_0 = 10^{-\mathrm{Slope}} - 1 \quad \textbf{12}$$

and

$$N_{max} = 10^{\mathrm{Intercept}} \quad \textbf{13}$$

This provides mathematical support for the analogy of the initial amplification efficiency (E_0) as is defined by Equation 8, to the slope-derived efficiency (E_S) as defined by a C_t-based standard curve (18). Indeed, this contention is borne out by the close correlation observed between E_0 and E_S values derived for each amplicon (Table 4; Supplementary Datasets 1 and 2).

Analogy with a C_t-based quantification can be extended further by substituting N_{max} for N_t in Equation 9, and converting amplicon number to reaction fluorescence:

$$F_{max} = F_0(E_0+1)^{C_{1/2}} \quad \textbf{14}$$

Table 4. Initial versus slope-derived estimates of amplification efficiency

Predicted N_0[a]	K3/K2 E_0[b] (%)	K1/K2 E_0[b] (%)
4.17×10^7	90.5	89.2
4.17×10^6	90.2	89.2
4.17×10^5	90.8	90.1
4.17×10^4	90.3	88.2
4.17×10^3	90.2	89.4
4.17×10^2	90.4	89.2
Average (%) ± SD (%)[c]	90.4 ± 0.2	89.2 ± 0.6
$C_{1/2} - E_S$[d]	89.8	91.0
$C_t - E_S$[e]	89.8 ± 2.1	90.0 ± 2.2

[a]Predicted number of target molecules based upon dilution of DNA standard quantified via A_{260}.
[b]Initial amplification efficiency (Equation 8).
[c]Average ± SD.
[d]Slope-derived estimate of amplification efficiency obtained from Figure 3.
[e]Slope-derived estimate of amplification efficiency obtained from C_t-based standard curves (18). See text for additional details.

from which two potentially useful derivatives can be obtained:

$$C_{1/2} = \mathrm{Log}_{(E_0+1)}\left(\frac{F_{max}}{F_0}\right) \quad \textbf{15}$$

and

$$E_0 = 10^{[\log(F_{max}/F_0)]/C_{1/2}} - 1. \quad \textbf{16}$$

Of practical significance is that Equation 16 provides an alternative method for calculating initial amplification efficiency when a quantified DNA standard is amplified, which can provide confirmation of E_0 values generated by Equation 8 (Supplementary Datasets 1 and 2).

DISCUSSION

Real-time PCR is well suited for high-throughput quantification of nucleic acids that could greatly benefit a variety of applications in medical diagnostics and genomics research, to name only two prominent fields. Large-capacity microtiter plates, combined with software automation of data collection and processing, provide the fundamental capabilities required for high-volume analysis. Nevertheless, high-throughput quantification is still technically difficult to achieve, primarily due to deficiencies of the threshold-based methodologies that have prevailed since the introduction of real-time PCR (1).

Most of these limitations center on the requirement for a reliable estimation of amplification efficiency that is generally acquired through construction of a standard curve, a process that is repeated for each target sequence. The technical challenges are not only exacerbated by difficulties of preparing quantified standards for each target, but also by the necessary assumption that the amplification efficiency of samples is identical, or at least similar, to that predicted by the standard curve. Such an assumption has been reported to be patently invalid for many cases in which amplification efficiency of samples has been determined (21,22). Not only can small differences in amplification efficiency produce large quantitative errors, the frequency and magnitude of these errors are virtually impossible to ascertain using a threshold approach.

The study described here extends the pioneering work of Liu and Saint (17), demonstrating that SCF can circumvent many of these deficiencies. The outstanding capabilities of SCF center on mathematic modeling of individual amplifications, which requires no prior assumptions other than dependency on the optical precision of the instrumentation. From this work, three aspects of practical significance are evident: quantification without prior knowledge of amplification efficiency, assessment of amplification efficacy and establishment of quantitative scale.

The effectiveness of SCF-based quantification is fundamentally linked to curve-fitting of experimental data, such that variations unique to each amplification reaction are incorporated into the analysis. Thus, instead of deriving a single quantitative entity, as is the case for threshold methodologies, SCF generates values for three kinetic parameters from which target quantity is calculated. Although lacking scale, the resulting target quantity could be directly used for relative quantification (16,23,24), with the advantage that determination of amplification efficiency is unnecessary.

This is not to say that amplification efficiency is unimportant, nor is it necessarily difficult to determine via SCF; indeed, amplification efficiency and target quantity are simply different expressions of the same kinetics parameters. Consequently, SCF allows the routine evaluation of amplification efficacy within individual reactions via monitoring of the initial amplification efficiency. In addition to identification of aberrant reaction preparation, this could allow detection of enzymatic inhibitors within the sample. Although effective quality control is clearly desirable for high-throughput applications in research, it is of even greater importance to biomedical diagnostics where reliability of analysis is paramount. It is equally evident that accuracy-of-scale is critical to many diagnostic applications, particularly for those involving pathogenesis and residual disease (5).

Of the many issues encompassing quantitative real-time PCR, provision of quantitative scale has some of the most profound implications, and yet it is one of the least understood. The simplicity of concept provided by standard curves employed under the threshold approach has likely contributed to the general oversight that quantitative scale is directly linked to amplicon fluorescence through its relationship to DNA mass. Based upon this principle, it was previously proposed that a common quantitative scale could be established for C_t-based analyses via determination of amplicon mass at threshold (18), a concept that was utilized further in this study. The relationship of quantitative scale to amplicon fluorescence is more evident under SCF in that target quantification is derived in fluorescence units. Determination of target copy number thus simply requires a calibration factor that relates fluorescence to DNA mass. It is the method for establishing this calibration factor, and the general effectiveness of applying a single calibration factor to multiple amplicons, that have major implications for the accuracy and reliability that can be achieved.

In this regard, it is important to note that optical calibration determines the absolute accuracy or 'exactness' of quantitative scale, whereas the curve-fitting process determines the precision of the assay (25). Although subtle, this is an important distinction in that acquisition of quantitative scale may be linked to PCR amplification (and thus susceptible to the factors impacting the precision of PCR quantification), but not necessarily so. Alternative methods for optical calibration can be envisaged that are independent of PCR, similar, for example, to the standard curves generated for DNA quantification using a dedicated fluorometer.

Equally significant is that once a calibration factor is established, it can provide a common quantitative scale for any target sequence, if it is assumed that the base pair composition and amplicon size do not significantly impact the fluorescence characteristics of SYBR® Green I. Under such an approach, the need for preparing a quantified DNA standard for each individual target sequence would be circumvented, and would allow large numbers of different targets to be quantified simultaneously, based upon a single, pre-established quantitative scale. Ultimately, it may be possible to introduce a 'gold standard' for the establishment of quantitative scale, which would further increase the utility and accuracy of quantitative real-time PCR.

In conclusion, SCF provides many of the fundamental capabilities required for fully automated high-throughput quantification that are lacking under currently employed methodologies. These include routine assessment of amplification efficacy within individual amplification reactions and elimination of PCR-generated standards curves, which when combined with provision of quantitative scale via optical calibration could allow reliable high-throughput quantification with minimal intervention. Based upon redefining the mathematics of PCR, sigmoidal modeling also elaborates more clearly on the theoretical aspects of PCR amplification upon which to base further investigations into the factors impacting amplification kinetics, and to more effectively expand the application of quantitative real-time PCR.

SUPPLEMENTARY MATERIAL

Supplementary Material is available at NAR Online. Supplementary Dataset 1: K1/K2 amplicon Excel workbook containing the fluorescence reading, SCF analysis and data summaries of the K1/K2 amplifications. Supplementary Dataset 2: K3/K2 amplicon Excel workbook containing the fluorescence reading, SCF analysis and data summaries of the K3/K2 amplifications.

ACKNOWLEDGEMENTS

The author thanks Brian Boyle and Richard Hamelin for their critical review of the manuscript, and Isabelle Lamarre for editorial assistance. This research was supported by a grant from the National Biotechnology Strategy of Canada.

REFERENCES

1. Higuchi,R., Fockler,C., Dollinger,G. and Watson,R. (1993) Kinetic PCR analysis: real-time monitoring of DNA amplification reactions. *Biotechnology*, **11**, 1026–1030.
2. Morrison,T.B., Weis,J.J. and Wittwer,C.T. (1998) Quantification of low-copy transcripts by continuous SYBR Green I monitoring during amplification. *BioTechniques*, **24**, 954–962.
3. Kang,J.J., Watson,R.M., Fisher,M.E., Higuchi,R., Gelfand,D.H. and Holland,M.J. (2000) Transcript quantitation in total yeast cellular RNA using kinetic PCR. *Nucleic Acids Res.*, **28**, e2.

4. Bustin,S.A. (2000) Absolute quantification of mRNA using real-time reverse transcription polymerase chain reaction assays. *J. Mol. Endocrinol.*, **25**, 169–193.
5. Niesters,H.G.M. (2001) Quantitation of viral load using real-time amplification techniques. *Methods*, **25**, 419–429.
6. Mackay,I.M., Arden,K.E. and Nitsche,A. (2002) Real-time PCR in virology. *Nucleic Acids Res.*, **30**, 1292–1305.
7. Ivnitski,D., O'Neil,D.J., Gattuso,A., Schlicht,R., Calidonna,M. and Fisher,R. (2003) Nucleic acid approaches for detection and identification of biological warfare and infectious disease agents. *BioTechniques*, **35**, 862–869.
8. Klein,D. (2002) Quantification using real-time PCR technology: applications and limitations. *Trends Mol. Med.*, **8**, 257–260.
9. Bustin,S.A. (2002) Quantification of mRNA using real-time reverse transcription PCR (RT–PCR): trends and problems. *J. Mol. Endocrinol.*, **29**, 23–39.
10. Wittwer,C.T., Herrmann,M.G., Moss,A.A. and Rasmussen,R.P. (1997) Continuous fluorescence monitoring of rapid cycle DNA amplification. *BioTechniques*, **22**, 130–138.
11. Wittwer,C., Ririe,K. and Rasmussen,R. (1998) Fluorescence monitoring of rapid cycle PCR for quantification. In Ferré,F. (ed.), *Gene Quantification*. Birkhäuser, Boston, MA, pp. 129–144.
12. Freeman,W.M., Walker,S.J. and Vrana,K.E. (1999) Quantitative RT–PCR: pitfalls and potential. *BioTechniques*, **26**, 112–125.
13. Pfaffl,M.W. and Hageleit,M. (2001) Validities of mRNA quantification using recombinant RNA and recombinant DNA external calibration curves in real-time RT–PCR. *Biotechnol. Lett.*, **23**, 275–282.
14. Rasmussen,R. (2001) Quantification on the LightCycler. In Meuer,S., Wittwer,C. and Nakagawara,K. (eds), *Rapid Cycle Real–Time PCR: Methods and Applications*. Springer Press, Heidelberg, pp. 21–34.
15. Lehmann,U. and Kreipe,H. (2001) Real-time PCR analysis of DNA and RNA extracted from formalin-fixed and paraffin-embedded biopsies. *Methods*, **25**, 409–418.
16. Peirson,S.N., Butler,J.N. and Foster,R.G. (2003) Experimental validation of novel and conventional approaches to quantitative real-time PCR data analysis. *Nucleic Acids Res.*, **31**, e73.
17. Liu,W. and Saint,D.A. (2002) Validation of a quantitative method for real time PCR kinetics. *Biochem. Biophys. Res. Commun.*, **294**, 347–353.
18. Rutledge,R.G. and Côté,C. (2003) Mathematics of quantitative kinetic PCR and the application of standard curves. *Nucleic Acids Res.*, **31**, e93.
19. Tichopad,A., Dzidic,A. and Pfaffl,M.W. (2002) Improving quantitative real-time RT–PCR reproducibility by boosting primer-linked amplification efficiency. *Biotechnol. Lett.*, **24**, 2053–2056.
20. Wilhelm,J., Pingoud,A. and Hahn,M. (2003) Validation of an algorithm for automatic quantification of nucleic acid copy numbers by real-time polymerase chain reaction. *Anal. Biochem.*, **317**, 218–225.
21. Meijerink,J., Mandigers,C., van de Locht,L., Tönnissen,E., Goodsaid,F. and Raemaekers,J. (2001) A novel method to compensate for different amplification efficiencies between patient DNA samples in quantitative real-time PCR. *J. Mol. Diagn.*, **3**, 55–61.
22. Ståhlberg,A., Åman,P., Ridell,B., Mostad,P. and Kubista,M. (2003) Quantitative real-time PCR method for detection of B-lymphocyte monoclonality by comparison of kappa and lambda immunoglobulin light chain expression. *Clin. Chem.*, **49**, 51–59.
23. Livak,K.J. and Schmittgen,T.D. (2001) Analysis of relative gene expression data using real-time quantitative PCR and the $2^{-\Delta\Delta Ct}$ method. *Methods*, **25**, 402–408.
24. Pfaffl,M.W. (2001) A new mathematical model for relative quantification in real-time RT–PCR. *Nucleic Acids Res.*, **29**, e45.
25. Ferré,F. (1998) Key issues, challenges, and future opportunities in gene quantification. In Ferré,F. (ed.), *Gene Quantification*. Birkhäuser, Boston, MA, pp. 1–16.